Accepted Manuscript

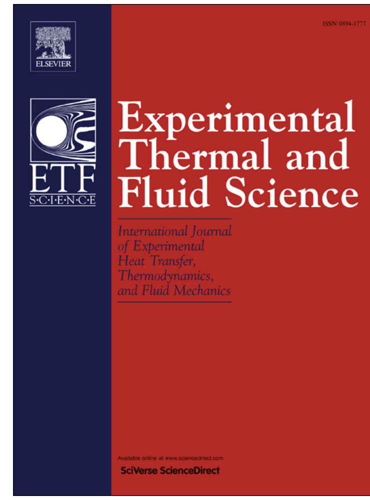

Toward the design of low flow-rate multijet impingement spray atomizers

M.R.O. Panão, J.M.D. Delgado

PII: S0894-1777(14)00167-8
DOI: http://dx.doi.org/10.1016/j.expthermflusci.2014.07.003
Reference: ETF 8262

To appear in: *Experimental Thermal and Fluid Science*

Received Date: 26 November 2013
Revised Date: 6 June 2014
Accepted Date: 1 July 2014

Please cite this article as: M.R.O. Panão, J.M.D. Delgado, Toward the design of low flow-rate multijet impingement spray atomizers, *Experimental Thermal and Fluid Science* (2014), doi: http://dx.doi.org/10.1016/j.expthermflusci.2014.07.003

Toward the design of low flow-rate multijet impingement spray atomizers

M.R.O. Panão[a,b], J.M.D. Delgado[b]

[a] *ADAI-LAETA, Mechanical Engineering Department*
University of Coimbra
Rua Luis Reis Santos, 3030-788 Coimbra, Portugal
[b] *Instituto Superior Técnico*
Technical University of Lisbon
Av. Rovisco Pais, 1049-001 Lisboa, Portugal

Abstract

When setting the baseline for discussing options toward a more efficient use of water resources, one of the drivers for decoupling economic growth and environmental impact is the development of resource-efficient innovations and instruments. One of such fields of interest is the design of water efficient showerheads, which provide a good shower experience, while consuming low flow rates (< 3l/min), and potentiating energy savings for heating water. As a step forward in this challenge, the approach followed in this work is motivated by the need to develop tools for designing tailored sprays toward a high degree of efficiency in water usage. However, in order to design tailored sprays, it is important to establish a proper relation between the atomizer's geometric configuration, operating conditions and the desired characteristics for the spray droplets (size and velocity). Therefore, this work focus on this tailoring through a multijet impingement atomization strategy using 2 and 3 impinging jets. An investigation is reported on the parametric effects on the dynamic characteristics of droplets of jet-impingement angle (40°- 90°) and pre-impingement distances (2.5 - 7.5 mm), for a range of jet Weber numbers ($20 < \mathrm{We}_j < 500$). The size of droplets is measured by image analysis, and their velocity by a Particle Tracking Velocimetry algorithm. The results evidence the similarities between droplet characteristics of sprays produced by 2- and 3-impinging jets, although the geometric effects induced by the jets' impingement angle are more relevant for the 3-impinging jets spray, while negligible for the 2-impinging jets spray. Moreover, empirical correlations for the arithmetic (d_{10}) and Sauter (d_{32}) mean diameters, normalized by the jet diameter (d_j), as well as drop velocity normalized by the jet velocity (u_d/u_j) are devised as tools for designing tailored multijet impingement sprays for low-flow rate water applications.

Keywords: multijet impingement spray, high-speed visualization, Particle Tracking Velocimetry, empirical correlations

1. Introduction

Multijet impingement atomization can be argued as a strategy with the advantage of producing tailored sprays through an appropriate design of the atomizer. Also, compared with free jet atomization, it enables liquid mixing and requires lower injection pressure at nozzle exit to obtain a certain drop size, for example, relatively to the free jet strategy applied in Diesel sprays. The multijet spray is produced from the single point coincidence of two or more cylindrical jets, forming a liquid sheet. This later further destabilizes in its bounding rim into ligaments, or interacts with the surrounding air in such a way as to detach into ligaments. These further fragment into droplets, thus constituting the spray. Most of the research performed in this atomization

ACCEPTED MANUSCRIPT

strategy is focus on the impingement of two jets [1]. But, one may wonder whether there are any advantages, or not, if more than two jets are considered to produce the spray. In previous works, multijet sprays produced with 2, 3 and 4-impinging jets have been applied for thermal management [2, 3, 4], and drop dispersion patterns have presented some geometric features, depending on the number of impinging jets [5], which is a feature distinguishing these sprays from the usual ones based on circular, annular or eliptical patterns. Moreover, the characteristics of droplets (size and velocity) did not appear to change significantly between the impingement of two, and more than two jets, requiring more fundamental work to provide further insight into the hydrodynamics underlying the atomization process using more than two jets. This is one of the aims of the present work considering the impingement of 2 and 3 jets.

The work here follows a previous one [6] and is also aimed at finding the tools toward a proper design of tailored multijet sprays, which depends on the characterization of droplets dynamics (size and velocity) and what are the effects of geometry and operating conditions on these characteristics. The common approach to develop these tools is to devise appropriate correlations between design parameters and droplets' mean characteristics. This will be briefly reviewed in the following subsection. Afterwards, section 2 describes the experimental setup, as well as the method used to characterize drop size and velocity. The following section contains the analysis of the results and discusses them from the point of view of liquid sheet morphology, and droplets characteristics, taking into account some of the theoretical work reviewed in section 1.1. The empirical approach to characterize drop size is taken into account and analyzed to retrieve further insight into the underlying physics of multijet atomization. A similar analysis is done for droplet velocity, rarely considered in the literature. The paper ends with some concluding remarks containing the general effects of geometry and operating conditions on the outcome of multijet atomization made with 2 and 3 impinging jets.

1.1. Empirical correlations for droplet characteristics

In order to design tailored multijet sprays, it is important to establish a proper relation between the atomizer's geometric configuration, operating conditions and the desired characteristics for spray droplets (size and velocity), in order to develop appropriate tools. Usually, these take the form of empirical correlations for mean drop size, and there are several approaches to its modeling in multijet impingement sprays. One of the first empirical correlations for the Sauter mean diameter (d_{32}) reported by Dombrowski and Hooper [7] is expressed as

$$\frac{d_{32}}{d_j} = \frac{4}{u_j^{0.79} \sin \theta^{1.16}} \tag{1}$$

where d_j and u_j are the jet diameter and average velocity and θ is the half-impingement angle. This correlation has been derived considering a normalized pre-impingement distance of $l_{pi}/d_j = 4$, $\mathrm{We}_j \in [370; 2635]$ and $2\theta \in [50°; 140°]$. The powers associated with u_j and θ are different to account for the influence the later has on the former, as well as on the liquid sheet thickness. In Tanasawa *et al.* [8], instead of considering variations of the jet impingement angle, different jet diameters (d_j) are taken into account (0.4-1mm), thus obtaining the correlation for a jets impingement angle comparable to [7]

$$\frac{d_{32}}{d_j} = \frac{1.73}{\rho_a^{0.1}} \mathrm{We}_j^{-1/4} \tag{2}$$

with σ, and ρ as the liquid surface tension and density, respectively, and ρ_a as the density of the surrounding environment. Recently, a dimensionless empirical approach has been proposed by Durst et al. [9] where the Sauter mean diameter is normalized by the jet's diameter and empirically correlated with a function of the half-impingement angle $f(\theta)$ and a function of both Ohnesorge ($\mathrm{Oh}_j = \mu/\sqrt{\rho\sigma d_j}$) and Reynolds numbers ($\mathrm{Re}_j = \rho u_j d_j/\mu$), $g(\mathrm{Oh}_j, \mathrm{Re}_j)$, generally expressed as

$$\frac{d_{32}}{d_j} = a \cdot g(\mathrm{Oh}_j, \mathrm{Re}_j) \cdot f(\theta) \tag{3}$$

On the one hand, the aforementioned correlations are relevant in the sense that d_{32} is a mean diameter expressing the relation between the volume and surface of a droplet, which is particularly important when heat transfer processes are considered. On the other hand, for the arithmetic mean diameter (d_{10}), based on a sheet instability analysis delineated by Dombrowski and Hooper [10], Ryan *et al.* [11] have presented a correlation for turbulent liquid jets expressed as

$$d_{10} = \left(\frac{2.62}{\sqrt[3]{12}}\right)\left(\frac{\rho_a}{\rho}\right)^{-1/6} (\mathrm{We}_j \cdot f(\theta))^{-1/3} \tag{4}$$

where We_j is the Weber number ($= \rho u_j^2 d_j/\sigma$), and $f(\theta)$ is a function given by $f(\theta) = (1 - \cos(\theta))^2/\sin(\theta)^3$. Despite Ryan *et al.* [11] have limited the empirical approach by opting for a dimensional format, the result is interesting in the sense that it points to the weak inverse dependence on the scaling parameter $\mathrm{We}_j f(\theta)$.

Other empirical correlations can be found in Ashgriz [1], generally involving parameters related with the jet diameter and velocity, and the half-jet-impingement angle θ. However, the jet velocities in these correlations are usually high, implying that these correlations are limited to operating conditions where atomization mechanisms often depart from the turbulent liquid sheet category.

1.2. Brief theoretical considerations

A more theoretical model for predicting the size distribution of droplets has been devised from the early analysis on the aerodynamic disintegration of viscous liquid sheets by Dombrowski and Johns [12], considering the growth rate of instabilities in long waves. Through a mass balance between a drop and the fraction of ligament from which it is generated, droplet size can be expressed as a function of liquid properties and the diameter of that ligament fraction (d_L) as

$$\frac{d_d}{d_L} = \left(\frac{3\pi}{\sqrt{2}}\right)^{1/3} \left[1 + \frac{3\mu}{\sqrt{\rho\sigma d_L}}\right]^{1/6} \tag{5}$$

Based on a non-linear model for impinging jet atomization, Ibrahim and Outland [13] suggested that ligaments disintegrate from the liquid sheet twice per wavelength and that the sheet thickness at breakup is $2h$, thus $\frac{\pi}{4}d_L^2 = \frac{1}{2}\lambda(2h) \iff d_L = \sqrt{\frac{8h}{k}}$. If this result is included in the theoretical model developed by Dombrowski and Johns [12], the ligament characteristic diameter d_L is expressed as

$$d_L = 0.9614 \left[\frac{K^2\sigma^2}{\rho_a \rho u_j^4}\right]^{1/6} \left[1 + 2.60\mu\sqrt{\frac{K\rho^4 u_j^7}{72\rho^2\sigma^5}}\right]^{1/5} \tag{6}$$

where K is the thickness parameter given by the product of the liquid sheet thickness h and the radial distance to the liquid sheet bounding rim r, which according to Hasson and Peck [14], considering an elliptic impingement region, results in

$$K = \frac{R^2 \sin\theta^3}{(1 - \cos\phi\cos\theta)^2} \tag{7}$$

or, if the impingement region is considered circular, according to Ibrahim and Przekwas [15], the thickness parameter becomes

$$K = \frac{R^2 \beta \exp\left(\beta(1 - \phi/\pi)\right)}{\exp(\beta) - 1} \tag{8}$$

where β is a coefficient determined by conservation of mass and momentum, and it is numerically determined according to [15] by

$$\cos\theta = \left(\frac{\exp(\beta) + 1}{\exp(\beta) - 1}\right) \frac{1}{1 + (\pi/\beta)^2} \tag{9}$$

In the visualization performed in this experimental work, a closer observation of the jet impingement region supports the approach of a circular impact. Moreover, it is noteworthy that applying eqs. (8) and (6) in (5), the variable parameters are the azimuthal angle ϕ, the jet velocity u_j and the half-impingement angle between the jets θ. A closer analysis of eq. (5) shows that the azimuthal angle evidences how droplets produced at $\phi = 0$ are estimated to be larger and that size tends to decrease as $\phi \to \pi$ corresponding to the top part of the liquid sheet. The jet velocity subtantially alters the maximum drop diameter at $\phi = 0$ and has a lesser influence when $\phi \to \pi$, thus being a scale parameter. The half-impingement angle alters the range of estimated drop sizes throughout the azimuthal range, namely decreasing

d_d at $\phi = 0$ and increasing it at $\phi = \pi$, thus it could be considered a shape parameter of the curve $d_d = f(\phi)$.

It is noteworthy that all these models consider ideal cases with a leaf-shape liquid sheet and no chaotic disruptions, e.g. holes inside the liquid sheet or in the bounding rim, as observed in the present experiments. Therefore, it is important that a more empirical analysis is developed toward devising tools for designing tailored multijet sprays in terms of defining drop sizes according to the geometric parameters chosen for the atomizer and operating conditions that depend on the application considered.

A final introductory note refers to droplet velocity, where very scarce information is found in the literature for multijet impingement sprays, although some authors report local measurements [5] or within a certain plane [16], but a correlation between the mean velocity of droplets and geometric parameters is still lacking.

2. Experimental setup and Diagnostic techniques

An experimental facility has been built to perform fundamental studies on multijet atomization up to the simultaneous impact of 4 jets, although the experiments reported in this work consider only the impact of two and three jets. The jets are formed using Pasteur pipettes with 1mm of inner diameter, thus, defining the jet diameter (d_j). Pipettes are assembled in a platform, which allows their movement with 4 degrees of freedom (x, y, z, θ), thus, enabling variations of the jet pre-impingement distance l_{pi} and angle of impact 2θ (Fig. 1).

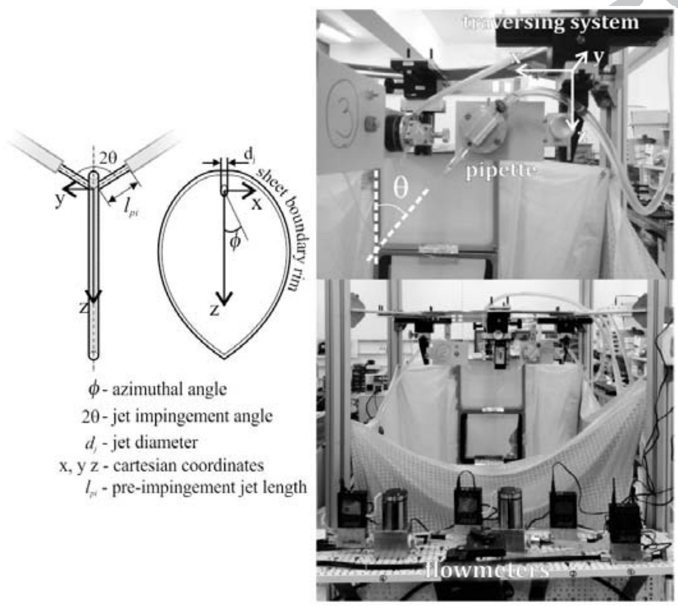

Figure 1: Parametric scheme of the two-impinging jets (left); Photo of experimental facility.

The experimental facility operates in a closed circuit, departing from a reservoir of water and distributing the overall volumetric flow rate by the pipettes, although the flow rate in each pipette is measured and controlled by ALICAT LCR and L flowmeters, up to a 2l/min range, with a precision of 0.01l/min. Finally, the reservoir is open at the top, thus, collecting the atomized fluid, as well as the excess water from the distributor.

The characterization of the atomization process is made with high-speed visualization using backlight LED illumination, and a high-speed camera Phantom v.4.3. Images of the flow are acquired at a frame rate of 2250 FPS covering an area of 512×512 pixel, corresponding to a resolution of 0.25-0.33mm/pixel. For the characterization of drop sizes, an image analysis software has been developed in Matlab using the pre-defined canny method to identify droplets boundaries. Since the shape of droplets produced is not always spherical, an equivalent diameter (d_d) is measured through the projected area A by $d_d = \sqrt{4 \cdot A/\pi}$, and a sphericity validation criteria of 90% is applied.

The characterization of droplet velocity is made using a Particle Tracking Velocimetry algorithm, as described in Vukasinovic *et al.* [17], where four consecutive images are analyzed to extract the velocity vector. Fig. 2 illustrates the algorithm followed in this work. For an image taken at t_i, a radius r_1 is set to 2 times a length scale defined by the time between two consecutive images and jet velocity ($u_j \cdot (t_{i+1} - t_i)$) and centered on a certain droplet i. For all droplets j within r_1 around droplet i, a velocity vector is calculated as $u_{d_{i,j}} = l_{i,j}/(t_{i+1} - t_i)$, where $l_{i,j}$ is the distance between droplet i and each droplet j. For all velocity vectors obtained, a search is made in the previous image $(i-1)$ and two images afterwards $(i+2)$, and the estimated location of droplet i is attempted within a smaller radius r_2 (0.3 of $u_j \cdot (t_{i+1} - t_i)$). If a droplet j is present in those locations, the corresponding velocity vector is validated. Fig. 3 shows the result of droplets velocity vector field obtained for two- and three impinging jets spray, and superimposes the four images analyzed.

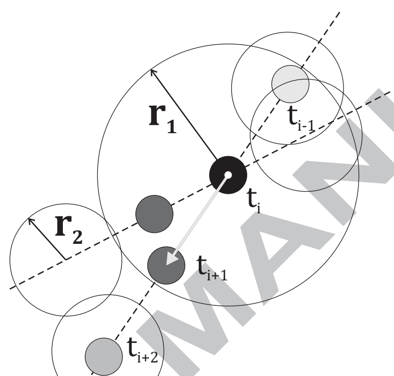

Figure 2: Illustration of the PTV algorithm that analyzes four consecutive frames in order to extract the velocity vector of each validated droplet (adapted fromVukasinovic *et al.* [17]).

The image processing results are analyzed using a classical statistical approach, in order to provide information of mean drop sizes and velocity. An error propagation analysis of the results presented produced maximum statistical errors for the size of less than 6% and less than 1% for the errors associated with droplet velocity. The experimental conditions consider water flow rates up to 0.6l/min, resulting in jet velocities of less than 6 m/s. Impingement angles (2θ) varied between 40° and 90° for both $N_j = 2$ and $N_j = 3$ impinging jets. Pre-impingement distances vary between 2.5 and 7.5

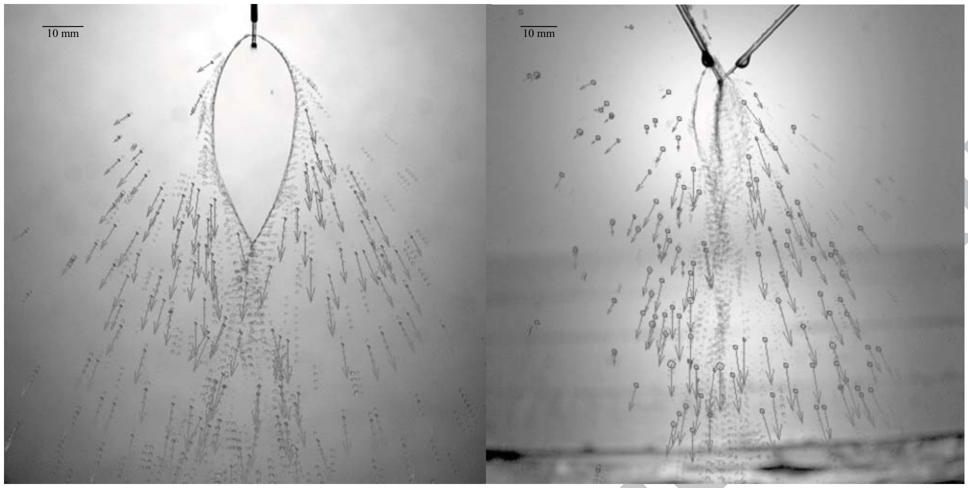

Figure 3: Example of droplets velocity vectors obtained by Particle Tracking Velocimetry in a superimposed image of the four used in the analysis. Left image obtained with 2-impinging jets, and the image on the right with 3-impinging jets.

of the jet diameter for both N_j configurations as well. The fluid is water and the experiments are performed under typical ambient conditions.

3. Results and Discussion

3.1. Hydrodynamic considerations on drop formation in 2- and 3-impinging jets sprays

It has been argued in previous works that the physics of atomization developed for sprays with $N_j = 2$ could be applied to sprays produced by more than 2 jets [5]. However, some differences have been measured and more fundamental work was required. Here, we will present some of the first fundamental experiments and a brief description of the differences between sprays with $N_j = 2$ and $N_j = 3$ in terms of sources of droplet formation.

With $N_j = 2$, the atomization occurs typically at the rim's boundary due to capillary instabilities (rim-droplets), as shown in the left of Fig. 4. If the We_j is higher, due to the interaction between the liquid sheet and the surrounding environment, inner-holes may appear in the liquid sheet, leading to the rim's disruption, and consequently, shortening the breakup length of the liquid sheet, forming detached ligaments that further fragment into droplets (detached droplets), as shown on the right of Fig. 4.

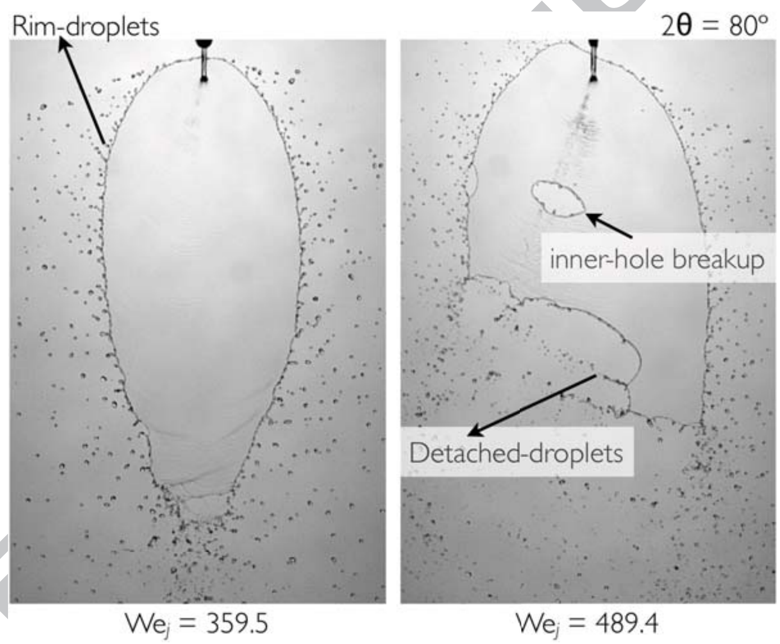

Figure 4: Typical sources of droplet formation in $N_j = 2$ multijet impingement sprays.

With $N_j = 3$, the hydrodynamic structure of the liquid sheet is tri-dimensional with the liquid sheet developing in the space between the jets in a half-leaflike shape (Fig. 5). While a 2-impinging jets spray is able to form smooth liquid sheets, those formed with 3-impinging jets appear to be more sensitive to instabilities propagating from the jets impact point, thus a ruffle structure is always present in all experimental conditions. Droplets have mainly three sources: the main one from the rim bounding the liquid sheet (rim-droplets), similar to $N_j = 2$; a second source emerges from an upward jet formed in the upper boundary at $\phi = \pi$ (upward-jet droplets); and a third source corresponds to a few bigger droplets formed from detached ligaments at $\phi = 0$. The image on the left of Fig. 5 provides an idea of the velocities of these droplets categories.

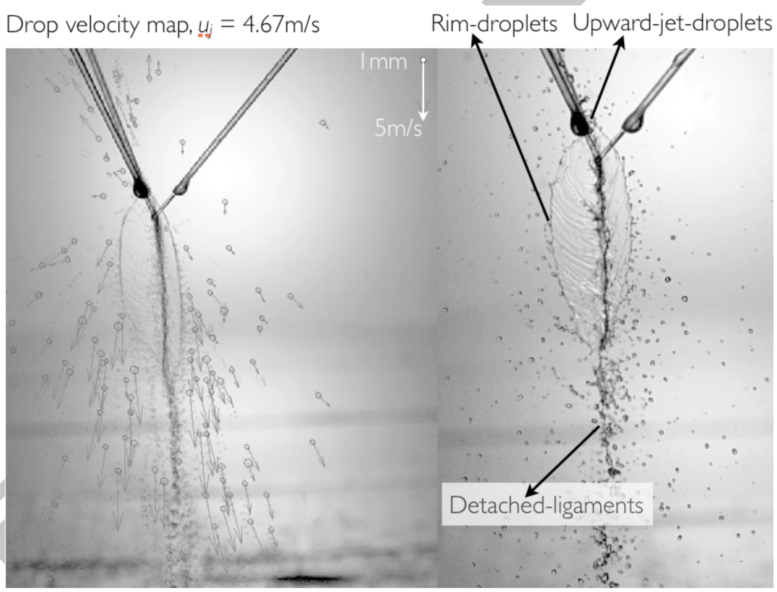

Figure 5: Typical sources of droplet formation in $N_j = 3$ multijet impingement sprays (right) and a corresponding example of droplet velocity map (left), $2\theta = 80°$, $l_{pi} = 5$ and $\mathrm{We}_j = 302.2$.

It is observed that rim-droplets have the highest velocities and upward-jet droplets are relatively slower. Droplets emerging from detached ligaments are only a few and not always detected because of the sphericity criterion imposed in the validation procedure. The following section analyzes the results obtained for the charaterization of droplets' size and velocity, and their correlation with operating and geometric parameters. The purpose is to gain some physical insight into the atomization process.

3.2. Correlation between drop size and operating/geometric parameters

It is noteworthy, prior to any analysis, that literature on sprays produced by impinging jets is still in its early stage of development for more than two impinging jets. Considering this, the main parameters usually correlated with drop size are the jet velocity and size (through the jet Weber number, We_j), and the half-jet-impingement angle θ (see Fig. 2). If we consider the results obtained in the experiments reported for the mean drop size, relatively to We_j and θ, one is able to observe in Fig. 6 that the mean drop size does not significantly vary between the sprays produced by 2- or 3-impinging jets. However, two stages are distinguished in terms of droplet characteristics. Namely, an intense decrease of drop size occurs until $\mathrm{We}_j \approx 100 - 150$, followed by a stage with a nearly stabilization of that size, regardless of the impingement angle.

The reason for these stages is associated with the kind of liquid sheet formed after jet impact. Fig. 7 shows a typology of the morphological changes in the liquid sheet with the impingement angle for a pre-impingement distance of $l_{pi}/d_j = 5$ and $\mathrm{We}_j = 249.7$ for the sprays with $N_j = 2$ and 3 impinging jets. The liquid sheet developing in the spaces between the jets is illustrated in Fig. 7 where the arrows indicate the jet flow direction.

For smaller impingement angles ($2\theta < 80°$), in most cases, instabilities

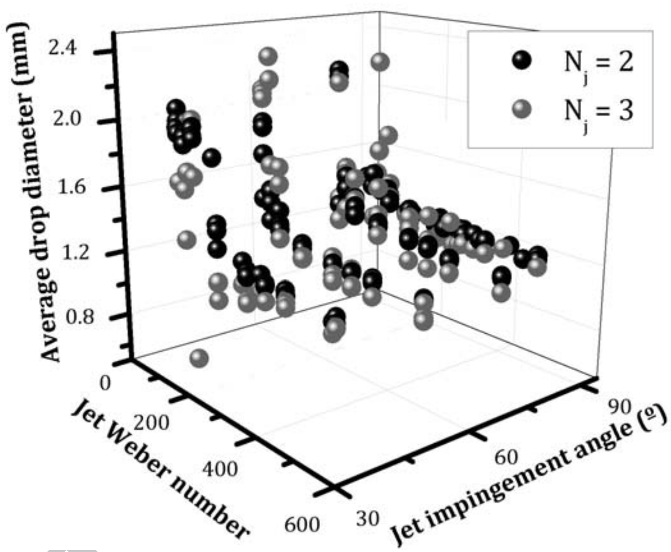

Figure 6: Correlation between mean drop size and operating conditions expressed by Wej and atomizer geometry expressed by jet impingement angle 2θ for 2- and 3-impinging jets sprays.

are observed inside the liquid sheet produced with $N_j = 2$, as the result of perturbations propagating from the point of impact due to a shear instability present in the water jet [18]. However, these instabilities are more commonly observed when $N_j = 3$ for the range of impingement angles used in the experiments. Also, when the impingement angle is smaller, the liquid sheet rim usually forms at the bottom end ($\varphi = 0°$) a corrugated ligament that disrupt into large droplets further downstream, and eventually, into satellite ones (Fig. 7, $2\theta = 40°$).

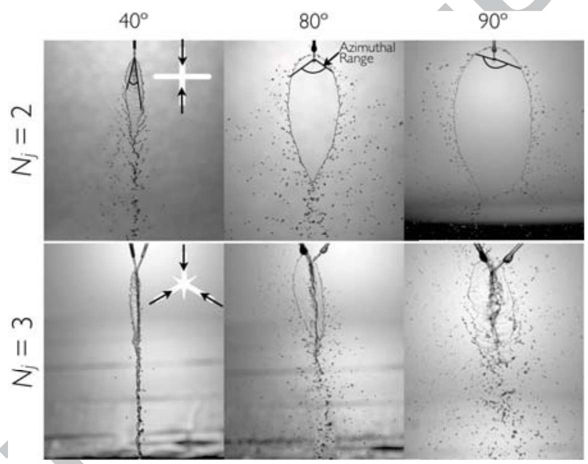

Figure 7: Typology of liquid sheet morphology as a function of the jet impingement angle ($l_{pi}/d_j = 5$; $\mathrm{We}_j = 249.7$).

With $N_j = 2$, a larger impingement angle (Fig. 7, $2\theta = 80°$) leads to the formation of a leaf-like shape liquid sheet with droplets emerging from ligament detaching at azimuthal locations approaching the top of the liquid sheet at $\varphi = \pi$. However, with $N_j = 3$, besides a similar observation, also the number of droplets appears to increase, which could be associated with the larger flow rate due to the introduction of one more jet.

Furthermore, although explored in more detail in the next section, the azimuthal range in the examples depicted in Fig. 7 for $N_j = 2$ indicates the location from which ligaments are detached, and later fragment into the spray droplets, and it is observed that it grows with the impingement angle. Thus, one may ask whether this has any influence over the average drop size of droplets. To make this assessment we consider the drop size range given by the theoretical model described in eq. (5), despite being formulated for $N_j = 2$. In this model, the maximum drop size (at $\varphi = 0$) and minimum ($\varphi = \pi$) establish the theoretical limits of maximum and minimum expected droplet size. For the angles considered in the examples given in Fig. 7 of the liquid sheet morphology, Fig. 8 depicts the average drop size obtained for $2\theta = 40°$, $80°$ and $90°$, considering $N_j = 2$ and 3, including the theoretical limits given by eq. (5).

In the case of $2\theta = 40°$, drop size is within the azimuthal range theoretically expected. A noteworthy observation is that, at $\mathrm{We}_j \approx 150$, a transition appears to occur in both $N_j = 2$ and 3, toward droplets with an average smaller size. The fact that there is no significant change between the sizes of droplets produced with 2- or 3-impinging jets suggests that the atomization mechanisms generating droplets do not depend on the number of impinging jets.

The different stages leading to the transition observed at $\mathrm{We}_j \approx 150$ in the mean diameter of droplets are visualized in Fig. 8b, for $2\theta = 80°$, where changes in the liquid sheet hydrodynamic structure between the two cases with similar We_j are evidenced for a normalized pre-impingement length of 5. The images on the left in Fig. 8b show droplets formed from the fragmentation of corrugated ligaments detaching at the bottom $\varphi = 0$ through a mechanism similar to a mix of Rayleigh and wind-induced breakup regimes [19]. However, theoretically, the fact that drop size is nearly independent of $\mathrm{We}_j (\geq 150)$, implies that most droplets are formed increasingly closer to the characteristic size of droplets emerging at $\varphi = 0$ theoretical limit.

3.3. Correlation between drop velocity and operating/geometric conditions

The velocity of droplets is determinant, *e.g.* to investigate the potential effect of their impact on the skin surface in the case of water applications, such as showers. Fig. 9 shows the correlation between the average drop velocity (u_d), normalized by the jet velocity (u_j), and the jet Weber number We_j, considering different pre-impingement jet lengths normalized by the jet diameter (l_{pi}/d_j) for $N_j = 2$ and 3.

While with $N_j = 2$, spray droplets have a larger average velocity, relatively to the jet velocity ($u_d/u_j > 1$), monotonically decreasing as a function of We_j, with $N_j = 3$, an increase of the impingement angle leads to a systematic decrease of the normalized drop velocity toward values lower than u_j. The pre-impingement jet length appears to induce a small variability in the results for the range of jet impingement angles considered $2\theta \leq 90°$.

The hypothesis advanced for explaining the evolution of u_d/u_j is related with the liquid sheet velocity. Droplets are formed from the fragmentation of ligaments detaching from the liquid sheet, thus, the velocities of both droplets and ligaments are likely to be related. It is also reasonable to think that the velocity of ligaments depends on the azimuthal coordinated in the liquid sheet at which detachment occurs. In this sense, the average drop velocity ultimately depends on the velocity of the liquid sheet. Choo and

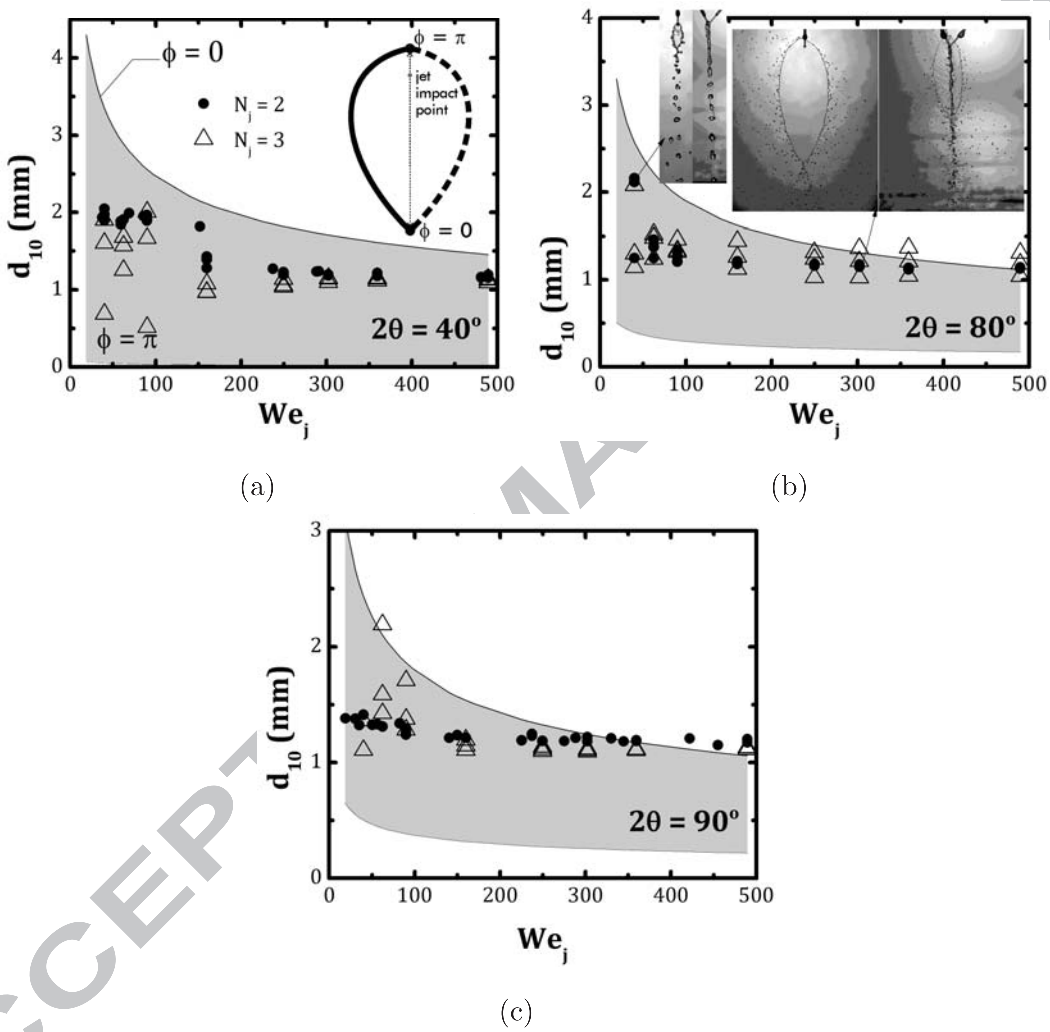

Figure 8: Analysis of the average drop size d_{10} within the azimuthal bandwidth of drop size range predicted as a function of jet Weber number We_j.

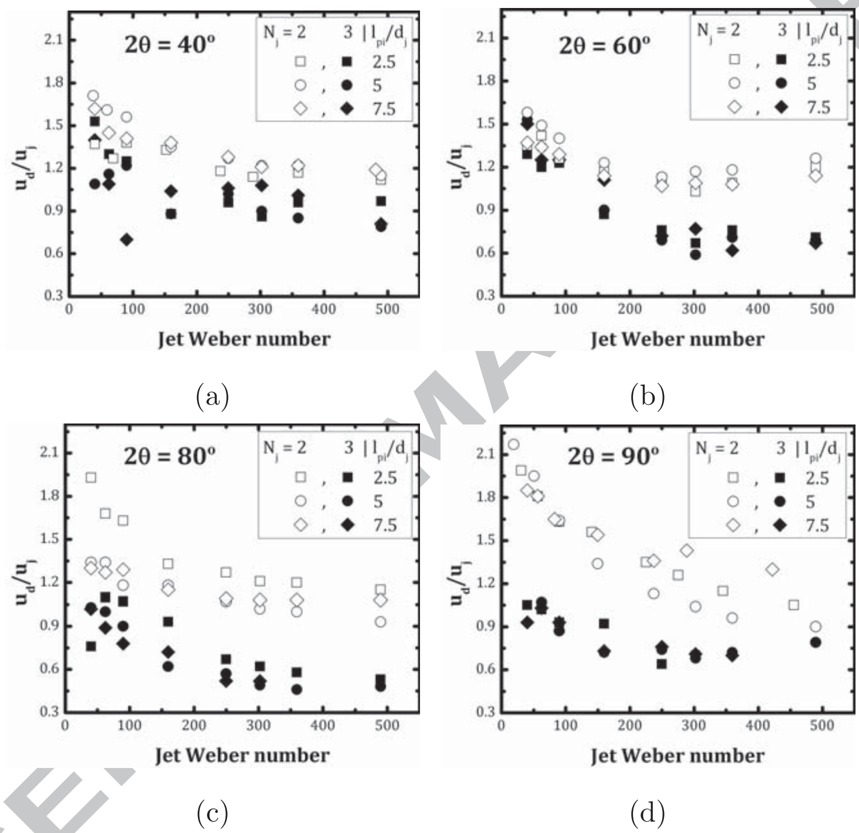

Figure 9: Average droplet velocity as a function of jet Weber number for different pre-impingement distances and jet impingement angles (40° - 90°).

Kang [20] have provided experimental evidence for the relation between the liquid sheet velocity (u_s) and jet velocity (u_j). Fig. 10 contains some of that data depicting u_s/u_j as a function of We_j for several azimuthal coordinates considering an impingement angle between jets of $2\theta = 140°$. It also indicates, according to Choo and Kang [20], the evolution of maximum and minimum values of u_s/u_j if the impingement angle 2θ decreases toward the values used in this work.

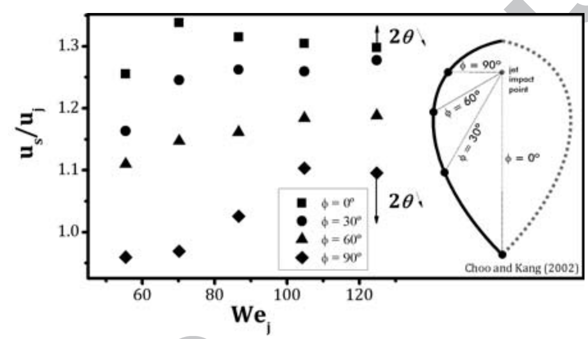

Figure 10: Variation of the ratio between liquid sheet and jet velocities, u_s/u_j, extracted from data reported by Choo and Kang [20], with $2\theta = 140°$.

Even if the values obtained for u_s/u_j were reported for a 140° jet impingement angle, the magnitude is similar to those reported in Fig. 9d for u_d/u_j. Thus, a possible explanation for the average decrease of u_d/u_j is that more droplets emerge from ligaments detached at higher azimuthal values φ, supporting the assumption that $u_d/u_j \to u_s/u_j$.

In fact, Fig. 11 shows for $2\theta = 80°$ that an increase in We_j is followed by a larger number of droplets detaching at higher azimuthal angles and, although not depicted, from $\mathrm{We}_j \approx 250$ onward, droplets practically emerge throughout the entire azimuthal range with both $N_j = 2$ and 3.

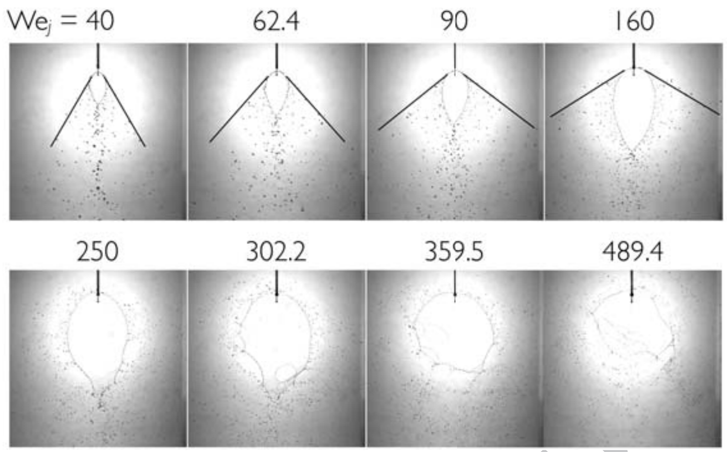

Figure 11: Increase of the number of droplets emerging at azimuthal coordinates $0 \leq \phi \leq \pi$ as a function of We_j.

3.4. *Tailoring multijet impingement sprays*

As mentioned in the introduction, a tailored spray implies the knowledge of the relation between the atomizer's geometric configuration, operating conditions and the desired characteristics for spray droplets (size and velocity). This can be expressed through empirical correlations, e.g. eqs. (1) - (4) devised for the mean size of droplets. Regarding eq. (4), it is reasonable to make two kinds of generalizations in the empirical approach. The first is to maintain the same structure and find the coefficients which best correlate with data:

$$d_{10} = a \cdot d_j \left(\mathrm{We}_j \cdot f(\theta)\right)^b \tag{10}$$

The other approach is to consider distinct exponents for We_j and $f(\theta)$:

$$d_{10} = a \cdot d_j \mathrm{We}_j^b \cdot f(\theta)^c \tag{11}$$

A similar approach is made for the correlation in eq. (3), where the Oh_j is included in constant a because d_j does not vary in our experiments, thus resulting in

$$d_{32} = a \cdot d_j \cdot \mathrm{Re}_j^b \cdot f(\theta)^c \tag{12}$$

Fig. 12 depicts the result obtained for the correlations of the Arithmetic (d_{10}) and Sauter (d_{32}) mean diameters devised for both $N_j = 2$ and 3. It has been verified that eq. (4) devised by Ryan et al. [11] provides reasonable results for $N_j = 2$ with a relatively low systematic error, or bias, and random (rnd) error. However, in terms of random error, the same is not observed for $N_j = 3$, where it is relatively high. This is a relatively expected outcome given that such correlations are devised for multijet sprays with $\mathrm{N}_j = 2$. Thus, this evidences the strong limitations of the later, if applied to an atomizer configuration with $\mathrm{N}_j > 2$, justifying the usefulness of the empirical approach here proposed for the design of multijet atomizers. On the other hand, eqs. (10) and (11) lead to better results for the experimental range considered, but the difference between approaches is mild for $N_j = 2$, while for $N_j = 3$, the bias and rnd errors slightly improve.

Relatively to d_{32}, both correlations of Dombrowski and Hooper [7] and Tanasawa et al. [8] fail by a major bias the results for the 2- and 3-impinging jets sprays evidencing the limitation of their assumptions to predict the size of droplets produced under low flow rate conditions. In both $\mathrm{N}_j = 2$ and 3 experiments, a proper fitting of arbitrary coefficients to experimental data using the approach of Durst et al. [9] provides empirical correlations for predicting the Sauter mean diameter of droplets with reasonable accuracy.

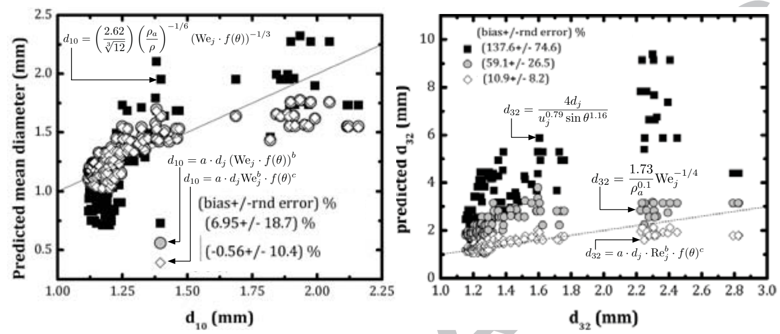

(a) $N_j = 2$

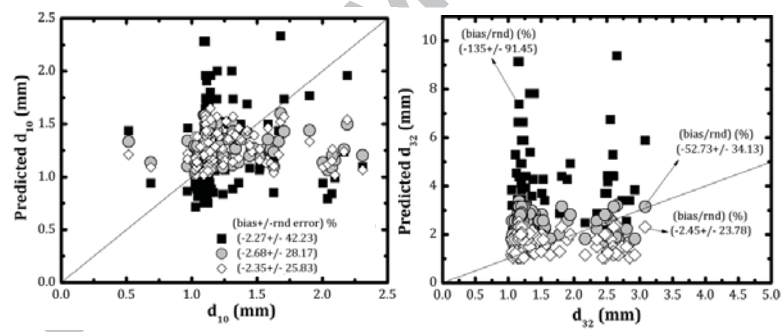

(b) $N_j = 3$

Figure 12: Correlation for the mean drop size as a function of the impingement angle $2\theta \leq 90^\circ$ and We_j.

The values of the correlation coefficients are summarized in Table 1. For the arithmetic mean diameter, the correlations that best describe the experimental results obtained evidence an even weaker dependence on the scaling parameter $\mathrm{We}_j f(\theta)$ (lower that 1/3 in absolute value). It is interesting to note that, while for $N_j = 2$ there is no difference between approaches comparing eqs. (10) and (11) as earlier remarked, for $N_j = 3$, the approach that independently considers the effects of operating conditions (expressed by We_j), and the geometry of the atomizer, $f(\theta)$,eq. (11), provides the best results, and, in so doing, the exponent associated with We_j becomes closer to that obtained with $N_j = 2$. This suggests that atomizing with 3 jets implies a greater dependence on geometric parameters relatively to $N_j = 2$, in this case through the jet-impingement angle (2θ). Furthermore, similar exponent values associated with We_j, for both impinging jets configurations, suggest that the influence imparted by jet dynamics on the formation of the liquid sheet that atomizes is also similar.

For the Sauter mean diameter (d_{32}), an analysis of the exponents indicates that the effect of both geometry and jet dynamics leads to a decrease of d_{32}, and the hydrodynamic impact of the impinging jets expressed by Re_j is relatively more important than the geometry of the atomizer expressed by $f(\theta)$, $|b| > |c|$. With the increase in the number of jets, an analysis of the exponents in the correlations for d_{32} also suggests that the greater effect associated with jet dynamics, compared to geometric effects, is slightly more pronounced. These are important considerations that should be taken into account in the design of multijet impingement sprays.

Finally, relatively to the correlation between drop velocity, normalized

N_j	Equation	a	b	c	R^2
d_{10}					
2, 3	(4)	3.5094	-1/3		0.6605, 0.2767
2	(10)	2.1407	-0.153		0.6293
	(11)	2.0795	-0.151	-0.1635	0.6324
3	(10)	1.8639	-0.125		0.2792
	(11)	3.0396	-0.157	0.0507	0.3499
d_{32}					
2	(12)	27.643	-0.4117	-0.2054	0.6287
3		220.1	-0.6406	0.1142	0.6062

Table 1: Correlation coefficient results for mean drop size.

by the jet velocity and the jet Weber number (We_j), for a wide range of geometric conditions (θ, l_{pi}), appropriate correlations are derived for each impinging jets configuration. For the first time, a useful empirical tool is provided for the design of tailored multijet impingement sprays.

It is noteworthy that also in the velocity, the effects induced by the geometry through $f(\theta)$ are important for $N_j = 3$, but not for $N_j = 2$. The fact that We_j has a negative exponent expresses what has already been analyzed in section 3.3, *i.e.* more droplets are being ejected at azimuthal locations where the resultant average velocity associated with the liquid sheet is lower. The residual values of the difference between data and the correlation results for $N_j = 2$ correspond to -0.59% of systematic error or bias and 10.9% of random error, while for $N_j = 3$, the bias is -1.22% and the random error is 16.5%.

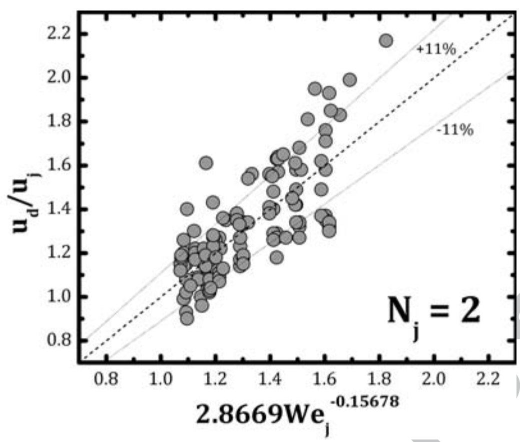

Figure 13: Correlation between the normalized drop velocity (u_d/u_j) for $N_j = 2$ with $R^2 = 0.6003$.

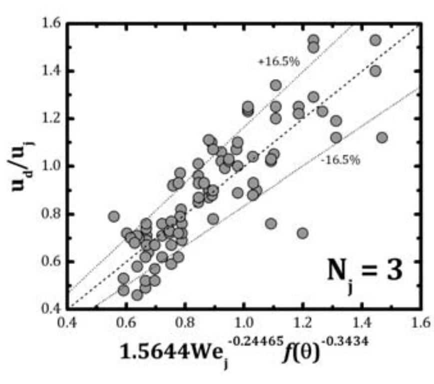

Figure 14: Correlation between the normalized drop velocity (u_d/u_j) for $N_j = 3$ with $R^2 = 0.7011$.

4. Concluding Remarks

In this work, a series of experiments are made to characterize droplets' size and velocity for a spray produced by the simultaneous impingement of two and three jets considering low flow rates (< 3l/min). The aim is to provide further insight into the relation between droplet dynamics, configuration and geometry of the atomizer for several operating conditions, and devise empirical correlations as design tools for producing tailored multijet impinging sprays. The geometrical configuration between jets considers impingement angles (2θ) in the range of $40°$ to $90°$, and pre-impingement jet lengths, normalized by the jet diameter ($d_j = 1$mm), ranging from 2.5 to 7.5. The Weber number of the jets (We_j) varies from 20 to 500. The characterization and comparison between atomizer configurations summarily evidence the following points:

- in both configurations ($N_j = 2$ and 3), smaller impingement angles lead to hydrodynamic structures characterized by larger drop sizes emerging from the breakup of a corrugated ligaments flowing from the bottom part of the liquid sheet centered on the azimuthal location of $\varphi = 0$;

- the average drop size is associated with the azimuthal location at which droplets are formed, defining the spray angle, and the mechanisms are observed to be similar between $N_j = 2$ and 3;

- while the effect of jet dynamics expressed by We_j in drop size and velocity is dominant in both sprays ($N_j = 2$ and 3), the effect of atomizer geometry, expressed as a function of the impingement angle, $f(\theta)$, is particularly relevant in the atomization process with $N_j = 3$;

- for $N_j = 2$ and 3, appropriate new empirical correlations under low flow-rate conditions have been devised for d_{10}, d_{32}, based on previous approaches reported in the literature, as well as for u_d/u_j.

Acknowledgments

The authors would like to acknowledge Fundação para a Ciência e Tecnologia (FCT) for the financial support of this work through the project MUST (PTDC/EME-MFE/099040/ 2008). Miguel Oliveira Panão would also like to acknowledge FCT for supporting his research through fellowship (SFRH/BPD/45170/2008).

References

[1] N. Ashgriz, Handbook of Atomization and Sprays, Springer-Verlag, 2011, Ch. Impinging Jet Atomization, pp. 605–707.

[2] M. Panão, A. Moreira, D. Durão, Thermal-fluid assessment of multijet atomization for spray cooling applications, Energy 36 (2011) 2302–2311.

[3] M. Panão, A. Correia, A. Moreira, High-power electronics thermal management with intermittent multijet sprays, Applied Thermal Engineering 37 (2012) 293–301.

[4] M. Panão, J. Guerreiro, A. Moreira, Microprocessor cooling based on an intermittent multijet spray system, International Journal of Heat and Mass Transfer 55 (2012) 28542863.

[5] M. Panão, A. Moreira, D. Durão, Transient analysis of intermittent multijet sprays, Experiments in Fluids 53 (2012) 105–119.

[6] M. Panão, J. Delgado, Effect of pre-impingement length and misalignment in the hydrodynamics of multijet impingement atomization, Physics of Fluid 25 (2013) 012105.

[7] N. Dombrowski, P. Hooper, A study of the sprays formed by impinging jets in laminar and turbulent flow, Journal of Fluid M 18 (1964) 392–400.

[8] Y. Tanasawa, S. Sasaki, N. Magai, The atomization of liquid by means of flat impingement, The Technology Reports of the Tohoku Univ. 22 (1957) 73.

[9] F. Durst, Y. Han, A. Handtmann, M. Zeilmann, Experimental and theoretical investigations of twin-jets, in: Proc. of the 12th Triennial Conf. on Liquid Atomization and Spray Systems, 2012.

[10] N. Dombrowski, P. Hooper, The performance characteristics of an impinging jet atomizer in atmospheres of high ambient density, Fuel 41 (1962) 323–334.

[11] H. Ryan, W. Anderson, S. Pal, R. Santoro, Atomization characteristics of impinging liquid jets, Journal of Propulsion and Power 11 (1995) 135–145.

[12] N. Dombrowski, W. Johns, The aerodynamic instability and disintegration of viscous liquid sheets, Chemical Engineering Science 18 (1963) 203–214.

[13] E. Ibrahim, B. Outland, A non-linear model for impinging jets atomization, Proc. IMechE 222 (2008) 213–224.

[14] D. Hasson, R. Peck, Thickness distribution in a sheet formed by impinging jets, AIChE Journal 10 (1964) 752–754.

[15] E. Ibrahim, A. Przekwas, Impinging jets atomization, Physics of Fluids A 3 (1991) 2981–2987.

[16] P. Vassalo, N. Ashgriz, F. Boorady, Effect of flow rate on the spray characteristics of impinging water jets, Journal of Prop 8 (1992) 980–986.

[17] B. Vukasinovic, M. Smith, A. Glezer, Spray characterization during vibration-induced drop atomization, Physics of F 16 (2004) 306–316.

[18] N. Bremond, E. Villermaux, Atomization by jet impact, Journal of Fluid Mechanics 549 (2006) 273–306.

[19] C. Baumgarten, Mixture formation in internal combustion engines, Springer, 2006.

[20] Y. Choo, B. Kang, The velocity distribution of the liquid sheet formed by two low-speed impinging jets, Physics of Fluids 14 (2002) 622–627.

Toward the design of low flow-rate multijet impingement spray atomizers

Miguel Oliveira Panão and João M. D. Delgado

HIGHLIGHTS

- Comparison between hydrodynamics of multijet atomisation with 2 and 3 impinging jets
- Drop size is closely related with azimuthal location of droplets formation
- Jet dynamics has similar influence in atomisation of 2- and 3-impinging jet sprays
- Atomizer geometry is particularly influential for 3-impinging jets sprays
- New empirical correlations for drop size and velocity are derived under low-flow rates